Spatially Resolved Collisional-Radiative Model for a Rarefied Plasma Plume

Bruno Fontaine[1 2 3(✉)], Federico Bariselli[1], Pietro Parodi[1 4], Pedro Jorge[1 5], Damien Le Quang[1], and Thierry Magin[1 2]

[1] von Karman Insitute for Fluid Dynamics, Aeronautics and Aerospace Department, Sint-Genesius-Rode, Belgium (bruno.fontaine@vki.ac.be)
[2] Université Libre de Bruxelles, Aéro-Thermo-Mécanique, Brussels, Belgium
[3] Université de Liège, Aérospatiale et Mécanique, Liège, Belgium
[4] KU Leuven, Department of Mathematics, Leuven, Belgium
[5] Vrije Universiteit Brussel, Materials and Chemistry, Brussels, Belgium

Abstract. The VKI DRAG-ON facility was designed to replicate Very Low Earth Orbit flow conditions, to study Air-Breathing Electric Propulsion intakes and gas-surface interaction physics. Its Particle Flow Generator produces a low-density, low-temperature argon plasma plume. This study investigates the flow's thermochemical non-equilibrium by comparing synthetic spectra from Collisional-Radiative modeling to Optical Emission Spectroscopy measurements. A Lagrangian reactor approach is used to account for the reacting species advection. Model-experiment comparisons reveal potential for plasma diagnostics and suggest targeted chemical model refinements. The results also show how the assumed Electron Energy Distribution Function shape can affect the diagnostics.

Keywords: optical emission spectroscopy, Lagrangian reactor

1 Introduction

The VKI DRAG-ON facility, commissioned in 2023, was designed to replicate the Very Low Earth Orbit (VLEO) flow conditions to study Air-Breathing Electric Propulsion (ABEP) [1] intakes and gas-surface interaction physics [7]. It operates in free molecular flow conditions, at pressures of the order of 10^{-5} mbar, using a LTA-100 Particle Flow Generator (PFG) from ThrustMe [12] to generate a partially ionized argon or oxygen plume with ion speeds of 6–10 km/s.

Since ion beams interact with walls through sheath potentials, as opposed to the mostly neutral flow at VLEO, corrections for wall effects require knowledge of the electron temperature and density. Characterizing these parameters is therefore essential for extrapolation to flight conditions. Optical Emission Spectroscopy (OES) is of particular interest for its simple setup and non-invasive nature. It provides line-of-sight (LoS) integrated emission intensities, which can be used to infer plasma parameters such as electron temperature and density [2, 9]. Their relation to the emission line intensities is established through a Collisional-Radiative (CR) model, describing the chemical reactions and radiative processes.

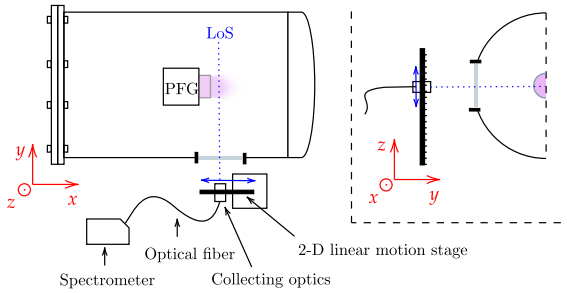

Fig. 1. Schematic experimental setup top view (*left*) and front view (*right*)

The CR model depends on the Electron Energy Distribution Function (EEDF) shape, which is often assumed to be Maxwellian. Other EEDF shapes can however be appropriate in some cases, including low-density plasmas [5, 6].

CR models are usually applied in a 0-D, Quasi-Steady-State (QSS) approach. However, for flows where chemical and flow timescales are comparable, the advection of the reacting species should be considered. A Lagrangian reactor approach provides an efficient alternative to a full flow-chemistry coupling, by transporting a thermochemical reactor along pre-computed streamlines without detailed chemistry, then recomputing the gas composition at each position [3].

In this study, we aim to advance the understanding of the non-equilibrium plasma dynamics in the VKI DRAG-ON facility by comparing spatially resolved OES measurements to predictions from a spatially resolved CR model using a Lagrangian reactor approach, for the PFG running with argon gas. We aim to identify the key factors influencing the model results and discrepancies with the experiment, such as electron temperature and density at the outlet of the PFG and the EEDF shape. In Sect. 2 we detail the experimental setup and OES data processing, in Sect. 3 we describe the modeling approach, and finally in Sect. 4 we compare results to assess model sensitivity and fidelity.

2 Optical Emission Spectroscopy

The DRAG-ON facility consists of two vacuum chambers linked by a duct that serves as test section for ABEP intake systems. Each chamber is equipped with a rotary vane mechanical pump and a turbomolecular pump, achieving an ultimate pressure of 10^{-8} mbar (when no gas is fed to the PFG). Each chamber is instrumented with hot-cathode and cold-cathode pressure gauges, and the main chamber has side windows for optical access. The PFG is aligned with the center axis of the main chamber (0.9 m length, 0.61 m diameter), and operated at 3 sccm argon flow, 60 W RF-power, 1 A focusing coil current, and floating electrode bias. During operation, the chamber pressure was 2.7×10^{-5} mbar.

Fig. 1 shows the OES setup. The light emitted by the plasma is collected with a 12 mm reflective collimator (RC12SMA-P01, ThorLabs) mounted on a 2-D

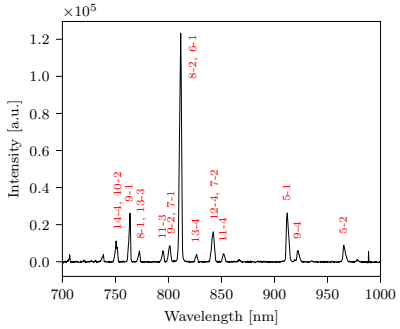

Fig. 2. Typical argon spectrum, at $x = 14$ mm and $z = 0$ mm

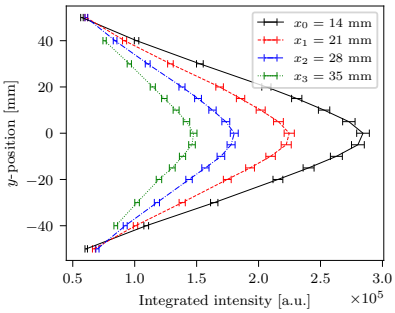

Fig. 3. Vertical intensity profiles (LoS integrated) for the line at 811 nm

motorized motion stage with 0.03 mm positioning accuracy. A 1 m optical fiber (MS53L01, ThorLabs) conducts the light to the high-sensitivity spectrometer (Maya2000Pro, OceanOptics) with a 600-1000 nm range, a circular aperture 50 µm in diameter, a blazed grating with 600 lines/mm, and a Hamamatsu S11510 CCD detector. The spectrometer was calibrated in wavelengths by the manufacturer. Relative intensity calibration was performed by replicating the setup in front of a black body source (R1500T, AMATEK Land) at 1723 K.

Spatial emission measurements were conducted by moving the optics relative to the plume's axis at the PFG outlet. Scans were performed at axial positions $x = 14$, 21, 28, and 35 mm, with a transverse step size of 5 mm up to $z = \pm 20$ mm, and a step of 10 mm beyond. The OceanView software was used for data acquisition. At each measurement point, 25 scans were performed for averaging, with 400 ms integration time each, with dark current correction.

Fig. 2 shows a typical spectrum, with background subtracted and setup spectral response correction. The emission lines are identified to argon transitions (red labels, with levels indexed by energy starting from the ground state Ar(0)). They are integrated spectrally for comparison to the CR model results. To reduce noise, they are fitted to a Gaussian, typical for instrumental broadening [2].

Fig. 3 shows the intensity spatial profiles for the 811 nm line. Others have similar profiles. The results show good symmetry and repeatability across campaigns. The uncertainty level, including fitting error and calibration noise, is small (average standard deviation of 3% and maximum of 10% for all lines, at all positions). The size of the window is a limitation of the current setup, as it prevents measurements far from the centerline, preventing Abel inversion.

3 Plume Model

The model predicts the intensity of emission lines by coupling a flow model with a Collisional-Radiative (CR) model using a Lagrangian reactor approach.

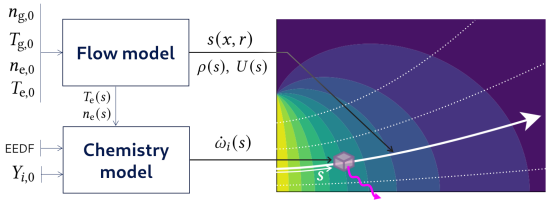

Fig. 4. Modeling approach and input parameters.

The governing equation for species conservation along streamlines is [3]:

$$\frac{\mathrm{d}Y_i}{\mathrm{d}s} = \frac{\dot{\omega}_i}{\rho U}, \quad \forall i \in \mathcal{S}, \tag{1}$$

where $\mathcal{S}$ is the set of species (here pseudo-species representing the excited states of argon), s (m) the curvilinear coordinate along the streamline, $Y_i = \rho_i/\rho$ (-) the mass fraction of species i, ρ (kg/m^3) the total mass density, U (m/s) the flow velocity norm, and $\dot{\omega}_i$ (kg/(m^{3}s)) the net chemical production rate of species i. The approach (Fig. 4) requires a *flow model*, which takes as inputs the conditions inside the PFG $n_{\mathrm{g},0}$, $T_{\mathrm{g},0}$, $n_{\mathrm{e},0}$ and $T_{\mathrm{e},0}$ respectively the neutral density, neutral temperature, electron density and electron temperature. Through the flow model, these inputs fix the streamlines and flow conditions along them. A *chemistry model* then recomputes the species concentrations according to Eq. (1) with a Lagrangian reactor advected along the streamlines starting from an initial distribution $Y_{i,0}$, with local reaction rates depending on the local electron temperature, electron density and shape of the EEDF.

Flow model: The plume is modeled as a collisionless thermal expansion of neutral argon, with analytical velocity and density fields [4], interacting with a field of hot electrons. The electron temperature and density fields were computed with a Particle-in-Cell (PIC) simulation of DRAG-ON [10], with uniform outlet conditions $T_{\mathrm{e},0} = 5$ eV and $n_{\mathrm{e},0} = 2 \times 10^{15}$ m^{-3}. For the purpose of this study, the results were extrapolated to different outlet conditions with a linear scaling.

CR model: It includes the 31 first energy levels of argon, extracted from the NIST Atomic Spectral Database (ASD) [8]. Neglecting heavy interactions and assuming the plasma to be optically thin, the reactions included in the model are electron impact excitation/de-excitation and spontaneous radiative decay:

$$\mathrm{Ar}(l) + \mathrm{e}^- \underset{K_{ul}}{\overset{K_{lu}}{\rightleftharpoons}} \mathrm{Ar}(u) + \mathrm{e}^-, \quad \mathrm{Ar}(u) \xrightarrow{A_{ul}} \mathrm{Ar}(l) + h\nu,$$

where $u > l$ are respectively the upper and lower states. Rate coefficients for radiative decay A_{ul} (s^{-1}) are extracted from NIST-ASD, selecting all allowed transitions involving levels in $\mathcal{S}$ with an experimentally observed wavelength and a known A_{ul} (77 reactions). Electron-impact rates K_{lu} (m^3/s) are computed as a weighted integral of cross sections with the EEDF, using cross sections from [13] (465 reactions). The integrals are pre-fitted to a modified Arrhenius form for

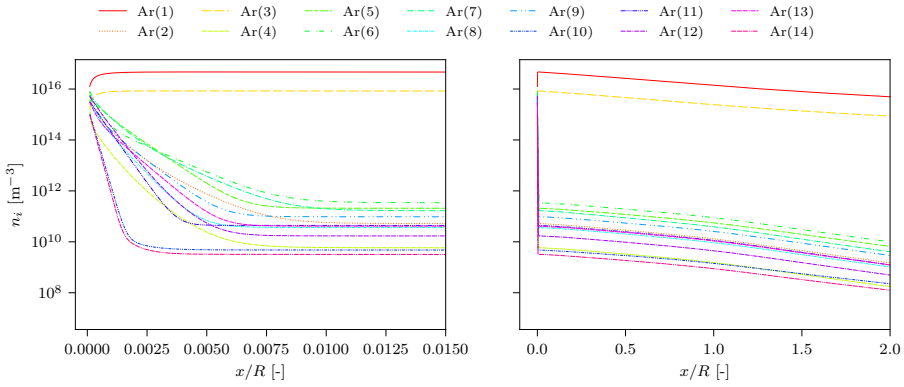

Fig. 5. Evolution of the densities of the 14 first excited states (centerline), with $n_{\mathrm{g},0} = 10^{19}$ m^{-3}, $T_{\mathrm{g},0} = 500$ K, $n_{\mathrm{e},0} = 5 \times 10^{14}$ m^{-3}, $T_{\mathrm{e},0} = 10$ eV, Maxwellian EEDF

efficiency. The de-excitation coefficients K_{ul} are computed with the principle of detailed balance. Finally, the net production rate for each level i is:

$$\dot{\omega}_i/M = \sum_{i<j} A_{ji} n_j - \sum_{i>j} A_{ij} n_i + \sum_{j\neq i} K_{ji} n_\mathrm{e} n_j - \sum_{j\neq i} K_{ij} n_\mathrm{e} n_i. \tag{2}$$

with $M = 6.63 \times 10^{-26}$ kg the atomic mass of argon.

Solving Eq. (1) along a streamline gives the evolution of excited-state populations. Fig. 5 shows results for the centerline, for typical input parameters. The initial conditions are chosen as a Boltzmann distribution at $0.2 \times T_{\mathrm{e},0}$ to start from a high state of excitation, as expected in the PFG ionization chamber.

We identify two main regions in the flow. First is a radiative length scale ($s/R < 0.015$), where the highly excited configuration from the PFG quickly decays, except for Ar(1) and Ar(3), the known argon metastables. After that, the flow appears to be chemically frozen, with a constant distribution of excited states along the streamline. For other plasma conditions than shown in Fig. 5, we also note a reactive length scale that appears in-between these two regions, of varying length depending on the T_e and n_e distributions.

4 Comparison of Model and Experiment

In this section, we reconstruct the experimental results from the model results. A comparison criterion is defined to perform a sensitivity analysis on the inputs.

The line intensities for each transition considered are predicted in the model from the rate coefficient A_{ul} and the number density of the upper excited state n_u, with $I_{ul}(x,r) \propto A_{ul} n_u(x,r)/\lambda_{ul}$. For lines involving multiple transitions, contributions are summed. LoS-integrated model intensities are generated for the positions $x_i \in \mathcal{X}$ (axial positions with experimental data) by applying the

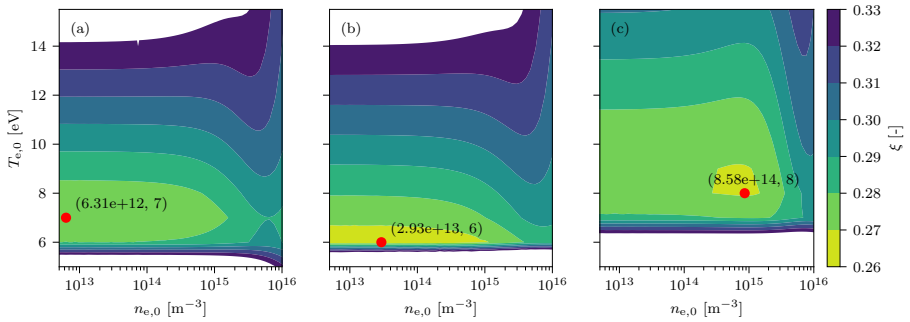

Fig. 6. Mapping of $\xi(n_{e,0}, T_{e,0})$ for each EEDF, with **(a)** Maxwellian, **(b)** Druyvesteyn and **(c)** Kappa ($\kappa = 2$), and location of minimum discrepancy ξ^* at $(T^*_{e,0}, n^*_{e,0})$.

forward Abel transform, assuming axisymmetry and the medium to be optically thin. OES intensities being relative, we normalize them with

$$\hat{I}_l^m(x,z) = \frac{I_l^m(x,z)}{\frac{1}{N_c}\sum_{x_i\in\mathcal{X}}\sum_{k\in\mathcal{L}} I_k^m(x_i,0)}, \tag{3}$$

where $m \in \{\text{OES,CR}\}$, l is the line index in set $\mathcal{L}$ of 12 identified lines, and $N_c = \sum_{\mathcal{X}}\sum_{\mathcal{L}} 1$ is the total number of intensity values measured on the centerline.

A comparison criterion ξ (-) is defined to quantify the discrepancy between the OES and model results:

$$\xi = \sqrt{\frac{1}{N}\sum_{l\in\mathcal{L}}\sum_{x_i\in\mathcal{X}}\sum_{z_j\in\mathcal{Z}_i} \frac{\left(\hat{I}_l^{\text{OES}}(x_i,z_j) - \hat{I}_l^{\text{CR}}(x_i,z_j)\right)^2}{\left(\hat{I}_l^{\text{OES}}(x_0,0)\right)^2}}, \tag{4}$$

with $\mathcal{Z}_i$ the set of z positions in the scan at x_i, and $N = \sum_{\mathcal{L}}\sum_{\mathcal{X}}\sum_{\mathcal{Z}_i} 1$ is the total number compared values. The resulting comparison criterion ξ is a function of the model parameters only, and equals zero for a perfect match.

A sensitivity analysis was performed on ξ with small perturbations to identify key parameters. The initial conditions $Y_{i,0}$ were parametrized using a Boltzmann distribution at $T_{el,0}$. The neutral density in the PFG $n_{g,0}$ is fixed as it only affects absolute intensities. The model showed low sensitivity to T_g ($\leq$1% variation between 300 and 600 K) or to $T_{el,0}$ ($\leq$7% between 1 and 15 eV, likely damped by the rapid radiative decay). However, higher sensitivity was found for the parameters governing electron impact excitation rates (EEDF shape, $T_{e,0}$, $n_{e,0}$). We therefore performed a mapping with respect to these parameters. The tested EEDF shapes were chosen to have very different tails (power-law for Kappa [11], exponential for Maxwellian, super-exponential for Druyvesteyn [5]).

Fig. 6 shows ξ maps over ($T_{e,0}$, $n_{e,0}$) for each EEDF. These maps could in principle reveal whether one EEDF shape leads to better agreement with the

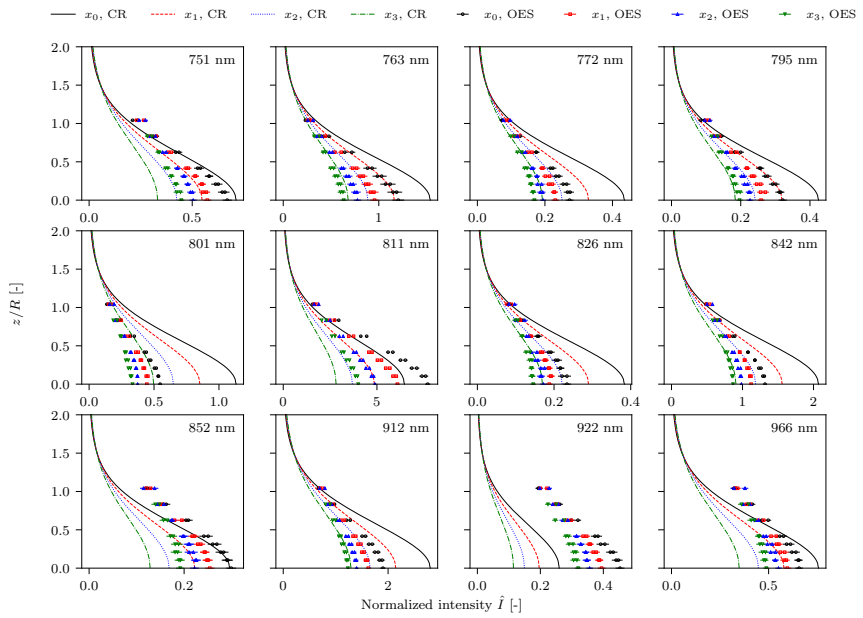

Fig. 7. Comparison of OES and model normalized intensity profiles for all lines, for a Kappa EEDF, $T^*_{e,0} = 8$ eV, $n^*_{e,0}$ =8.58×10^{14} m^{-3}, $T^*_{el,0} = 1.6$ eV, and $T^*_{g,0} = 500$ K

experiment. Here, however, all three yield similar minimum ξ^*. Nonetheless, the ξ contours differ depending on the choice of EEDF, and so does the location of the minimum discrepancy. In particular, we note that a less populated tail leads to a higher sensitivity on T_e. On the other hand, the sensitivity on n_e remains relatively low for all EEDF shapes.

The obtained estimates of the electron temperature $T^*_{e,0}$ identified in Fig. 6, aligns well with invasive measurements [7]. This supports the potential for non-invasive diagnostics in DRAG-ON. For the electron density, the optimal n^*_e values are scattered across several orders of magnitude depending on the used EEDF. The diagnostics of n_e is therefore not conclusive at this stage because of the low sensitivity of ξ and the correlation between n^*_e and the unknown EEDF shape. Fig. 7 shows a visual comparison of OES and CR normalized intensities for a Kappa distribution at the minimum discrepancy. It shows reasonable agreement, given the large model uncertainties, with Einstein coefficients uncertainties reaching 50% [8] and cross sections varying widely across databases, but shows the model can be further improved to reduce discrepancies.

5 Conclusions and Future Work

This study advances the understanding of non-equilibrium plasma dynamics in the VKI DRAG-ON facility by comparing the first spatially resolved OES mea-

surements in the facility to a CR model using a Lagrangian reactor approach. A promising first problem inversion identified an electron temperature in the expected range, demonstrating the potential of our approach for non-invasive diagnostics in DRAG-ON, which could ultimately be applied during ABEP intake tests or gas-surface interaction studies. Remaining discrepancies between model and experiment suggest future model improvements such as extended PIC databases for different PFG conditions and inclusion of radiation trapping by metastable states. Particular attention should also be given to assumptions on the EEDF. While the EEDF shape had little impact on the extracted electron temperature under the present test conditions, it did affect the sensitivity of the model to the electron temperature and the optimal electron density, suggesting that it remains a critical parameter for plasma diagnostics. Langmuir probe measurements or Boltzmann equation simulations could provide alternatives to the analytical shapes used here. Future work will also focus on plasma diagnostics by problem inversion with uncertainty quantification tools.

Acknowledgements: Bruno Fontaine is a F.R.S.-FNRS Research Fellow.

References

1. Andreussi, T., et al.: The AETHER project: development of air-breathing electric propulsion for VLEO missions. CEAS Space Journal 14(4), 717–740 (2022)
2. Bariselli, F., et al.: Characterization of an Air-Xenon Operated Electric Thruster Plume through Optical Emission Spectroscopy. In: 9th International Workshop on Radiation of High Temperature Gases for Space Missions. Azores, Portugal (2022)
3. Boccelli, S., et al.: Lagrangian diffusive reactor for detailed thermochemical computations of plasma flows. Plasma Sources Science & Technology 28(6), 065002 (2019)
4. Cai, C., Boyd, I.D.: Collisionless Gas Expanding into Vacuum. Journal of spacecraft and rockets 44(6), 1326–1330 (2007)
5. Druyvesteyn, M.J., Penning, F.M.: The mechanism of electrical discharges in gases of low pressure. Reviews of modern physics 12(2), 87–174 (1940)
6. Gudmundsson, J.T.: On the effect of the electron energy distribution on the plasma parameters of an argon discharge: a global (volume-averaged) model study. Plasma Sources Science & Technology 10(1), 76–81 (2001)
7. Jorge, P.D.C., et al.: Relevance of an RF plasma source to satellite material testing in VLEO conditions (2025), preprint available on Research Square. Under review at CEAS Space Journal.
8. Kramida, A., et al.: NIST Atomic Spectra Database (2022)
9. Lee, D., et al.: Two-dimensional electron temperature and density profiles of Hall thruster plume plasmas using tomographically reconstructed optical emission spectroscopy. Plasma Sources Science & Technology 31(12), 125004 (2022)
10. Parodi, P., et al.: Particle-in-Cell simulation of the VKI DRAG-ON facility. In: AIAA SciTech Forum (2024)
11. Pierrard, V., Lazar, M.: Kappa Distributions: Theory and Applications in Space Plasmas. Solar physics 267(1), 153–174 (2010)
12. Rafalkyi, D., Dudin, S.: RF Plasma Flow Generator for LEO Environment Simulation: Use Cases. In: 38th International Electric Propulsion Conference (2024)
13. Zatsarinny, O., Wang, Y., Bartschat, K.: Electron-impact excitation of argon at intermediate energies. Physical Review A 89(2) (2014)